ASTRONOMY
AND
ASTROPHYSICS

The heavy-element abundances of AGB stars and the angular momentum conservation model of wind accretion for barium stars

Y.C. Liang[1,3]**, G. Zhao**[1,3]**, and B. Zhang**[2,4]

[1] Beijing Astronomical Observatory, Chinese Academy of Sciences, Beijing 100012, P.R. China
[2] Department of Physics, Hebei Normal University, Shijiazhuang 050016, P.R. China
[3] National Astronomical Observatories, Chinese Academy of Sciences, Beijing 100012, P.R. China
[4] Chinese Academy of Sciences-Peking University Joint Beijing Astrophysical Center, Beijing 100871, P.R. China

Abstract. Adopting new s-process nucleosynthesis scenario and branch s-process path, we calculate the heavy-element abundances of solar metallicity $3M_\odot$ thermal pulse asymptotic giant branch (hereafter TP-AGB) stars, and then discuss the correlation between heavy-element abundances and C/O ratio. $^{13}C(\alpha, n)^{16}O$ reaction is the major neutron source, which is released in radiative condition during the interpulse period, hence gives rise to an efficient s-processing that depends on the ^{13}C profile in the ^{13}C pocket. A second small neutron burst from ^{22}Ne source marginally operates during convective pulses over previously s-processed material diluted with fresh Fe seed and H-burning ashes. The calculated heavy-element abundances and C/O ratio on the surfaces of AGB stars are compared with the observations of MS, S and C (N-type) stars. The observations are characterized by a spread in neutron exposures: 0.5-2.5 times of the corresponding exposures reached in the three zones of the ^{13}C pocket showed by Fig. 1 of Gallino et al. (1998). The evolutionary sequence from M to S to C stars is explained naturally by the calculated heavy-element abundances and C/O ratio.

Then the heavy-element abundances on the surfaces of TP-AGB stars are used to calculate the heavy-element overabundances of barium stars, which are generally believed to belong to binary systems and their heavy-element overabundances are produced by the accreting material from the companions (the former TP-AGB stars and the present white dwarfs). To achieve this, firstly, the change equations of binary orbital elements are recalculated by taking the angular momentum conservation in place of the tangential momentum conservation, and the change of $\delta r/r$ term is considered; then the heavy-element overabundances of barium stars are calculated, in a self-consistent manner, through wind accretion during successive pulsed mass ejection, followed by mixing. The calculated relationships of heavy-element abundances to orbital periods P of barium stars can fit the observations within the error ranges. Moreover, the calculated abundances of nuclei of different atomic charge Z, corresponding to different neutron exposures of TP-AGB stars, can fit the observational heavy-element abundances of 14 bar-ium stars in the error ranges. Our results suggest that the barium stars with longer orbital period $P>$1600 d may form through accreting part of the ejecta from the intrinsic AGB stars through stellar wind, and the mass accretion rate is in the range of 0.1-0.5 times of Bondi-Hoyle's accretion rate. Those with shorter orbital period $P<$600 d may be formed through other scenarios: dynamically stable late case C mass transfer or common envelope ejection.

Key words: nuclear reactions, nucleosynthesis, abundances – stars: abundances – stars: AGB and post-AGB – stars: carbon – stars: mass-loss – stars: binaries: close

1. Introduction

Since Burbridge et al. (1957) and Cameron (1957) published their pioneering studies, the nucleosynthesis theory has been developed in deep degree. In particular, TP-AGB stars are very important to study element nucleosynthesis and the Galactic chemical evolution because they synthesize significant parts of slow process (hereafter s-process) neutron capture elements and ^{12}C. The products are taken out from the stellar interior, He-intershell, to the surface by the third dredge-up (hereafter TDU) process, and then are ejected into interstellar medium with the progressive stellar wind mass loss.

Our understanding of the AGB nucleosynthesis has undergone major revisions in these years. The earlier studies (Iben 1975; Truran & Iben 1977) illustrated that intermediate mass TP-AGB stars with $^{22}Ne(\alpha, n)^{25}Mg$ neutron source (the typical neutron density is least of a order of $10^9 - 10^{10} n$ cm^{-3}) are the suitable nucleosynthesis sites of s-process elements. But new observations shed doubts on the above idea (Busso et al. 1995, 1999 and references therein). Busso et al. (1995) and Lambert et al. (1995) demonstrated that the measured abundances of Rb/Sr, the products of the branch in the s-process path at ^{85}Kr, imply a definitely lower neutron density (typical of the order of $10^7 n$ cm^{-3}), which can be provided via the reaction $^{13}C(\alpha, n)^{16}O$ at low temperature in the He-intershell of low mass AGB stars.

Iben & Renzini (1982a,b) indicated that a suitable mechanism operated in low mass stars of low metallicity to allow the formation of a semiconvective layer, hence the ^{13}C pocket. The pocket is engulfed by the next convective pulse where ^{13}C nuclei easily capture α nuclei, release neutrons. Hollowell & Iben (1988) confirmed the possibility of formation of a consistent ^{13}C pocket through a local time-dependent treatment of semiconvection. However, the semiconvection mixing mechanism was not found to work for the ^{12}C-enriched Population I red giants, like the peculiar stars of MS, S and C stars, showing overabundances of s-process elements in their spectra.

Straniero et al. (1995) investigated the effect of a possible mixing of protons into a thin zone at the top of the carbon-rich region during each dredge-up episode, hence the formation of ^{13}C pocket. They suggested that the ^{13}C was completely burnt in the radiative condition, and the resulting s-process nucleosynthesis occurs during the quiescent interpulse period, instead of the convective thermal pulse. ^{22}Ne$(\alpha, n)^{25}$Mg was still active for a very short period during the convective pulse with minor influence on the whole nucleosynthesis. Herwig et al. (1997) and Herwig et al. (1998) supported the formation of ^{13}C pocket via hydrodynamical calculations.

Straniero et al. (1997) adopted the above new s-process nucleosynthesis scenario to calculate the s-process nucleosynthesis of solar metallicity low mass AGB stars with $1 \leq M/M_\odot \leq 3$, and gave the detailed results.

Recently, Gallino et al. (1998) explained further and developed the aforesaid new scenario. They divided the ^{13}C pocket, q layer, into three zones in the light of the distribution in the mass of hydrogen introduced in the ^{12}C-rich intershell. The characteristic neutron exposures in the three layers are different. Moreover, when the nucleosynthesis occurs in a radiative layer, only the nucleosynthesis products are ingested into the convective thermal pulse, which makes the classical concept of mean neutron exposure (τ_0) become meaningless and the simple assumption of an exponential distribution of the neutron exposure fail to account for the complexity of the phenomenon (Arlandini et al. 1995; Gallino et al. 1998). Busso et al. (1999) reviewed this new s-process nucleosynthesis scenario in details.

The spectral and luminosity studies of AGB stars (including MS, S and N-type C stars) have shown that the M$\rightarrow$S$\rightarrow$C sequence is the result that the low-mass AGB stars have undergone carbon synthesis, s-process nucleosynthesis and the third dredge-ups (Lambert 1991). These stars are in the course of experiencing thermal pulse stage, and the original chemical abundances of their atmospheric envelope have been modified by two mixing mechanisms, namely, the first dredge-up when they became red giants and the third dredge-up when they became TP-AGB stars (Boothroyd & Sackmann 1988a, b, c and d).

The predicted evolutionary sequence of M$\rightarrow$S$\rightarrow$C in the heavier$-$lighter s-element abundances relationship (here and hereafter, 'heavier' refers to the second metal peak elements: Ba, La, Ce, Nd and Sm etc.; 'lighter' refers to the first metal peak elements: Y, Zr etc.) and the heavy-element abundances$-$C/O relationship (^{12}C, together with the s-process elements, is dredged up from stellar interior during the third dredge-up process) are important to understand the nucleosynthesis and evolution of AGB stars. Because (1) they will provide theoretical basis for the observed evolution of the sequence, (2) they can check the available theories on the evolutions of AGB stars (e.g., the beginning of the third dredge-up process, the mass and the chemical abundance of the dredge-up material, the theory of s-process nucleosynthesis, the stellar wind mass loss, and the formation of carbon stars etc.).

Busso et al. (1992) discussed the heavy-element abundances of M, MS and S stars using the thermal pulse AGB model. Busso et al. (1995) analyzed the heavy-element overabundances of carbon stars under the assumption that the dredge-up started after reaching the asymptotic distribution (about the 20th pulse). It is difficult to calculate the AGB stars evolution and s-process nucleosynthesis. So there are few theoretical results to explain the M$\rightarrow$S$\rightarrow$C evolutionary sequence based on the combination of the heavier$-$lighter s-element abundances ratio and the C/O ratio, though the observational abundances exhibit a certain regularity. Zhang et al. (1998a) calculated the evolution of the surface heavy element abundances and C/O ratio for a $3M_\odot$ TP-AGB star with initial metallicity 0.015, and gave interesting results. But they adopted mean neutron exposure τ_0 and unbranch s-process path, which have been revised in these years.

In the first part of this paper, we adopt the new s-process nucleosynthesis scenario (Straniero et al. 1995; Straniero et al. 1997; Gallino et al. 1998; Busso et al. 1999 etc.), and the branch s-process nucleosynthesis path to calculate the s-process nucleosynthesis of solar metallicity $3M_\odot$ AGB stars. And then, we discuss the M$\rightarrow$S$\rightarrow$C sequence based on the heavy-element abundances and C/O ratio.

The importance of AGB stars nucleosynthesis is not only to explain the observational M$\rightarrow$S$\rightarrow$C sequence but also to be responsible for the origin of some other classes of stars with overabundances of heavy-elements.

Observations revealed that some stars with overabundances of heavy-elements were not luminous to up to the stage of AGB. Following Lambert (1991), the stars showing heavy-element overabundances are divided into two classes: (1) intrinsic TP-AGB stars$-$they include MS, S and C (N-type) stars exhibiting the unstable nucleus ^{99}Tc ($\tau_{\frac{1}{2}} = 2 \times 10^5$ yr) as evidence that they are presently undergoing nucleosynthesis activity and the third dredge-up, and (2) extrinsic AGB stars$-$they include the various classes of G-, K-type barium stars and the cooler S, C stars where ^{99}Tc is not observed. It is generally believed that the extrinsic AGB stars belong to binary systems and their heavy-element overabundances come from accretion of the matter ejected by the companions (the former AGB stars, now evolved into white dwarfs) (McClure et al. 1980; Boffin & Jorissen 1988; Jorissen et al. 1998; Jorissen & Van Eck 2000; Jorissen 1999). The mass exchange took place about 1×10^6 years ago, so the ^{99}Tc produced in the original TP-AGB stars have decayed. The accretion may either be disk accretion (Iben & Tutukov 1985) or common envelope ejection (Paczynski 1976). Han et al. (1995) investigated in detail the evolutionary channels for the formation of barium stars. In this paper we will only discuss the stellar

wind accretion scenario because it is very important to explain the formation of barium stars (Boffin & Jorissen 1988; Jorissen et al. 1998).

Boffin & Jorissen (1988) calculated qualitatively the variation of orbital elements caused by wind accretion in binary systems. They also estimated the heavy-element overabundances of barium stars. Subsequently, Boffin & Začs (1994) used similar methods to calculate the overabundances, and interpreted the relationship between the heavy-element abundances and the orbital periods of barium stars.

Some important conclusions have been drawn in the theory of wind accretion, but the previous calculations on orbital elements were not very reliable because of the neglect of the $\delta r/r$ term (r represents the distance between the two components of the binary system), and using the tangential momentum conservation (Chang et al. 1997 and references therein). For the rotating binary system with wind mass loss, the total angular momentum conservation is more reasonable than tangential momentum conservation. Also, the previous calculations of heavy-element overabundances used the 'step-process' (Boffin & Jorissen 1988; Boffin & Začs 1994), which means that the overabundance factor changes at one single instant from 1 to f (f is the relative ratio of the heavy-elements to the solar abundances, and differs for different elements. Earlier calculations used the mean f value of carbon stars), and then keeps the value until the end of the AGB phase. However, after the start of the TDU, the overabundance factor f of the intrinsic AGB stars changes during successive dredge-ups. It is after a number of dredge-ups that the C/O ratio in the outer envelope of the intrinsic AGB star reaches 1, which means that the AGB star becomes a carbon star. The heavy-element overabundances of the barium star should be caused by the successive pulsed accretions and mixing.

According to the analysis to the orbital elements of barium and S stars, Jorissen & Mayor (1992) presented the evolutionary pathways of binaries leading to barium and S systems. They concluded that the binary systems with longer orbital period formed through wind accretion and those with shorter orbital period formed via Roche lobe overflow. But the specific range of orbital period was not presented. Jorissen et al. (1998) analyzed the orbital elements of a large sample of binary systems to give insight into the formations of barium and Tc-poor S stars. They suggested that barium stars with orbital period $P>1500$ d formed through wind accretion scenario. Zhang et al. (1999) suggested that the barium stars with $P>1600$ d formed via wind accretion according to their model. Liu et al. (2000) suggested that the barium stars with orbital period $P>1600$ d evolved from normal G, K giants through wind accretion scenario.

Besides the orbital elements, the heavy-element abundances of barium stars have been discussed in some literatures. Busso et al. (1995) discussed the observational heavy-element abundances of barium stars. And a more detailed analysis of the abundance distributions for five stars has been performed using the method of mixing the accretion mass with the envelope mass. But the effect of mass accretion and the changes of orbital elements were not considered. Chang et al. (1997) and

Liang et al. (1999) attempted to explore the relationships between the heavy-element overabundances and orbital elements of bariums stars using the binary accretion scenario, but with the shortcomings: or using the tangential momentum conservation, or adopting the old nucleosynthesis scenario of TP-AGB stars.

In the second part of this paper, we firstly calculate the variation equations of orbital elements based on the angular momentum conservation model of wind accretion, then we calculate the heavy-element overabundances of barium stars via successive pulsed accreting matter enriched heavy-elements from the intrinsic AGB stars, and mixing the matter with their envelopes.

This paper is organized as follows. The observational data of MS, S, C (N-type) stars and barium stars are given in Sect. 2. In Sect. 3, we present the model and the main parameters of AGB stars nucleosynthesis and the angular momentum conservation model of wind accretion scenario for barium stars. Sect. 4 illustrates and analyzes our results. We conclude and discuss in Sect. 5.

2. Observations

The abundance data of the heavy-elements, C and O elements of MS and S stars are taken from Smith & Lambert (1985, 1986, 1990). The listed values of [N/Fe] ($=\log(N/Fe)_{star}-\log(N/Fe)_{sun}$) have typical errors $0.1-0.2$ dex, and N represents a kind of s-process element. Indeed, for the observations in the series papers of Smith & Lambert, the accuracy of the iron peak elements (Ti, Fe and Ni) abundances and the heavy-elements Y, Zr, Nd abundances were better. But the abundance of Nd element is only at 50% of s-origin, it is not reasonable to regard Nd as the representative of heavier s-elements (Busso et al. 1992; Zhang et al. 1998a), and the reasonable representative should be the mean abundance of Ba, La, Nd and Sm elements (Busso et al. 1995). In order to do this we suggest that the initial abundance of Nd have to be increased by 0.11 dex before the data of MS and S giants are compared with carbon stars (Busso et al. 1995). Y and Zr elements are the representatives of lighter s-elements. For C and O elements, the accuracy is higher at 0.1 dex in Smith & Lambert (1990). Considering that, at present, the sample with both observed C/O ratios and heavy-element abundances is rather limited and there is a close relationship between the Tc-no MS, S stars (stars that contain no Tc) and the thermal pulse AGB stars (Busso et al. 1992; Jorissen & Mayor 1992), we can usefully include the Tc-no stars in our study of evolutionary tendency of the M→S→C sequence (Busso et al. 1992).

The abundance data of heavy-elements of the 12 carbon stars (N-type) are taken from Utsumi (1985), with typical errors of 0.4 dex in [N/Ti], which are dealt like in Busso et al. (1995). The corresponding abundances of C, O elements are taken from Lambert et al. (1986).

The heavy-element abundances of 12 barium stars are taken from Začs (1994). For ζ Cap and HR 774, the heavy-element abundances are from the same sources as in Busso et al. (1995). The sun, instead of ϵ Vir, is chosen to be a comparison standard, namely, [N/Fe]$=\log(N/Fe)_{star}-\log(N/Fe)_{sun}$. The abun-

dances of ϵ Vir to the sun are taken from Tomkin & Lambert (1986). The new solar system abundances are taken from Anders & Grevesse (1989). The overabundances of s-process elements in barium stars are characterized by a mean value of [s/Fe]=([Y/Fe]+[Ba/Fe]+[La/Fe]+[Ce/Fe]+[Nd/Fe])/5.0. The typical error is 0.2 dex (Boffin & Začs 1994). Zr has been excluded from this mean value, since the abundance of Zr is poorly related to other heavy-elements in the sample (Boffin & Začs 1994). The corresponding observational data of orbital elements, orbital period P and eccentricity e, are taken from McClure & Woodsworth (1990), Boffin & Začs (1994) and Jorissen et al. (1998).

3. The model and the main parameters

3.1. The nucleosynthesis and mixing in AGB stars

AGB star consists of three layers: a C-O core of degenerate electron, a He and H double burning shell, and a convective envelope. Heavy-elements synthesized in the He-intershell are dredged up to the convective envelope by the convection that appears in the cooling contraction after a thermal pulse, and show up as the observed overabundances of the heavy-elements and ^{12}C. With the evolution of the star, its core mass steadily increases with increasing thermal pulses, while the mass of the convective envelope decreases correspondingly via wind mass loss, until it is completely exhausted, while marks the life span of the thermal pulse AGB star.

During every thermal pulse, we calculate the s-process nucleosynthesis. ^{56}Fe is taken to be the seed nucleus for the s-process. The reaction ^{209}Bi(n,γ)^{210}Bi(α)^{206}Pb(^{210}Bi has an α-decay half-life of 5.01 days) terminates the reaction chain of the slow process of neutron capture. The branch s-process path is adopted in the calculation. The neutron capture cross sections of most of nuclei, are taken from Beer et al. (1992). The β-decay rates and electron capture rates of nuclei are taken from Takahashi & Yokoi (1987). More recent values of some nuclei are taken from the same literatures as those cited by Gallino et al. (1998). For the initial abundances, we use standard red giant abundances, which differ from the solar abundances only by a constant factor: $N_i = N_{i\odot} \times Z/Z_\odot$. At present, the solar system abundance distribution is the most detailed abundance distribution obtained by us. According to the results of Straniero et al. (1997) and Gallino et al. (1998), the main parameters adopted in calculation are as follows:

(1) Core mass   At the onset of the thermal pulse, the mass of the C-O core is $0.572M_\odot$. With successive pulses, both the H burning and He burning shells move outwards (in mass coordinates) and so does the C-O core. The core mass is up to $0.611M_\odot$ at the 8th pulse, during which the third dredge-up begins. The variation of the core mass influence directly the wind mass loss. The core masses of stars in different TP periods are taken from Table 4 of Straniero et al. (1997).

(2) Mass loss through wind   Wind mass loss is one of the most important ingredients in the computation of both the nucleosynthesis occurring in TP-AGB stars and the wind accretion on the secondary component of a binary system. Here, we adopt

the mass loss rates given by Straniero et al. (1997) using Reimers formula (Reimers 1975) based on the TP-AGB stellar models (their Table 4).

The mass lost during the time Δt, the interpulse period, is

$$\Delta M = -\dot{M}\Delta t, \tag{1}$$

which is taken from Table 4 of Straniero et al. (1997).

(3) Dilution Factor   The physical process that influences significantly the surface abundance is the third dredge-up. The dilution factor f is defined as the ratio of the mass dredged in every pulse to the mass of the envelope after the third dredge-up begins, namely,

$$f = \frac{\Delta M_{\mathrm{TDU}}}{M_{\mathrm{env}} + \Delta M_{\mathrm{TDU}}}, \tag{2}$$

where ΔM_{TDU} is the mass dredged up from He-intershell at every pulse since TDU begins, and M_{env} is the mass of the envelope. The cumulative effect of the various TDU, $\sum \Delta M_{\mathrm{TDU}}$, have been given in Fig. 9a of Gallino et al. (1998).

(4) Overlap factor   The overlap factor rr, $rr = 1 - \Delta M_{\mathrm{c}}/M_{\mathrm{CSH}}$, is the ratio of the number of a kind of nuclide that is exposed to neutron in two successive pulses to the number exposed in the previous pulse, that is, the overlap fraction of the convective shells between the two successive pulses. Where ΔM_{c} is the increment of the core mass during the previous interpulse period, and M_{CSH} is the mass of the convective inter-shell. The variation of rr with core mass was given by Iben (1977) and Renzini & Voli (1981). According to suggestion of Straniero et al. (1995), rr steadily decreases with increasing core mass. In this paper, we adopt the values given by Fig. 9c of Gallino et al. (1998).

(5) Neutron source ^{13}C$(\alpha, n)^{16}$O reaction is the major neutron source of s-process nucleosynthesis, which is released in radiative conditions at $T_8 \sim 0.9$ during the interpulse period, hence gives rise to an efficient s-processing that depends on the ^{13}C profile in the ^{13}C pocket, q layer. The layer is divided into three zones, in which the neutron exposures change with the various interpulse periods (Gallino et al. 1998, see their Fig. 6). Then the products of nucleosynthesis are ingested into the convective thermal pulse, and mixed with s-process material already from the previous pulses, and with the H-burning ashes from the below H shell. A second small neutron burst from the ^{22}Ne source operates during convective pulses due to the high neutron density and high temperature. The ^{22}Ne source to the total neutron irradiation is small, ranging from $\sim$0.002 mb^{-1} at the 9th pulse to $\sim$0.05 mb^{-1} in the latest pulses, where the average effective temperature is $\sim$23 keV.

(6) Light neutron poisons   Some isotopes can consume neutron produced by the neutron source isotopes, ^{13}C or ^{22}Ne, through some reactions. They are named as neutron poisons. For example, the isotope ^{14}N through its resonant channel ^{14}N$(n, p)^{14}$C, ^{26}Al in its long-lived ground state synthesized by the reaction ^{25}Mg$(p, \gamma)^{26}$Al^g (Gallino et al. 1998 and references therein). However, in the previous convective pulses, ^{14}N is destroyed in the reaction chain leading to ^{22}Ne production, and a large fraction of ^{26}Al has undergone substantial depletion by neutron capture. The above discussion makes it clear

that compared to a convective burning scenario, the radiative s-process is much less affected by the filtering effect of light neutron poisons (Gallino et al. 1998). So in the radiative s-process nucleosynthesis calculation, we neglect the influence of these light neutron poisons (the slightly effects on nucleosynthesis calculation caused by this will be further discussed in Sect. 4.1).

(7) Value of C/O   At the beginning of the AGB phase, the C/O on the surface of a low mass stars is approximately 0.31, and lower than the initial (solar) value (approximately 0.45) because it has been modified by the first dredge-up process, which reduces the ^{12}C abundance of the surface by about 30%. With the third dredge-up process, ^{12}C of He-intershell is mixed into the stellar surface with the mixing of s-process material. So the C/O ratio on the surface increases gradually. In calculation, we adopt the C/O ratio from Table 4 of Straniero et al. (1997).

3.2. The heavy-element overabundances of barium stars

3.2.1. The angular momentum conservation model of wind accretion

For the binary system, the two components (an intrinsic AGB star, the present white dwarf, with mass M_1, and a main sequence star, the present barium star, with mass M_2) rotating around the mass core C, so the total angular momentum is conservative in the mass core reference frame. If the two components exchange material through wind accretion, the angular momentum conservation of total system is showed by:

$$\Delta(\mu r^2 \dot{\theta}) = \omega r_1^2 (\Delta M_1 + \Delta M_2) + r_2 v (\Delta M_1 + \Delta M_2), \quad (3)$$

where μ is reduced mass, and r is the distance from M_2 to M_1. r_1, r_2 are the distances from M_1, M_2 to the mass core C respectively. ω ($=2\pi/P$, where $P=2\pi A^2 (1-e^2)^{\frac{1}{2}}/h$ is orbital period) is angular velocity. v is an additional effective velocity defined through the angular momentum variation in the direction of orbital motion of component 2. The first term on the right side of the equal-sign is the angular momentum lost by the escaping material, and the second term is the additional angular momentum lost by the escaping material.

Using the similar method to that adopted by Huang (1956), Boffin & Jorissen (1988) and Theuns et al. (1996), considering the angular momentum conservation of total system and not neglecting the square and higher power terms of eccentricity, we can obtain the change equations of the orbital elements:

$$\frac{\Delta A}{A} = -2(1-e^2)^{\frac{1}{2}} \left[\frac{\Delta M_1}{M_1} + \frac{\Delta M_2}{M_2} - \frac{\Delta M_1 + \Delta M_2}{M_2} \frac{v}{v_{\text{orb}}} \right]$$
$$+ 2(1-e^2)^{\frac{1}{2}} \frac{M_2(\Delta M_1 + \Delta M_2)}{M_1(M_1 + M_2)}$$
$$+ [2(1-e^2)^{\frac{1}{2}} - 1] \frac{\Delta M_1 + \Delta M_2}{M_1 + M_2}, \quad (4)$$

$$\frac{e\Delta e}{1-e^2} = [1 - (1-e^2)^{\frac{1}{2}}] \left[\frac{\Delta M_1}{M_1} + \frac{\Delta M_2}{M_2} - \frac{\Delta M_1 + \Delta M_2}{M_1 + M_2} \right]$$
$$- [1 - (1-e^2)^{\frac{1}{2}}] \frac{M_2(\Delta M_1 + \Delta M_2)}{M_1(M_1 + M_2)}$$

$$- \frac{3e^2}{2(1-e^2)^{\frac{1}{2}}} \frac{\Delta M_1 + \Delta M_2}{M_2} \frac{v}{v_{\text{orb}}}, \quad (5)$$

where A is the semi-major axis of the relative orbit of component 2 around 1, and e is the eccentricity (more details can be found in Appendix and Liu et al. 2000). Here, we take $v=0$ (Boffin & Jorissen 1988).

For the mass accreted by the barium star, we use the Bondi-Hoyle (hereafter B-H) accretion rate (Bondi & Hoyle 1944; Theuns et al. 1996; Jorissen et al. 1998):

$$\Delta M_2^{\text{acc}} = -\frac{\alpha}{A^2} \left(\frac{GM_2}{v_{\text{ej}}^2} \right)^2 \left[\frac{1}{1 + (v_{\text{orb}}/v_{\text{ej}})^2} \right]^{\frac{3}{2}} \Delta M_1, \quad (6)$$

where α is a constant expressing the accretion efficiency. Theuns et al. (1996) indicated that taking α between 0.5 and 1, as suggested by the numerical simulations of Ruffert & Arnett (1994), the actual accretion rate deduced from the smoothed particle hydrodynamics (hereafter SPH) simulation in the $\gamma = 1.5$ case was thus about 10 times smaller than that predicted by the B-H formula. Here we take $\alpha=1$ for the B-H formula. In fact, Boffin & Začs (1994) suggested that the actual accretion rate is between 0.1 and 1 times of B-H rate. We take 0.15 times of the B-H rate as the actual accretion rate for our standard case. v_{ej} is the wind velocity, and v_{orb} is the orbital mean velocity. After fixing the initial conditions, for the mass ΔM_1, ejected at each pulse by the primary star, we can solve the Eqs. (4)-(6) for ΔM_2, the accreted mass by the secondary star. And then, the heavy-element abundances on the surface of barium stars can be calculated.

3.2.2. The heavy-element overabundances of barium stars

The calculation is completed by two separated steps. Firstly, adopting the theory of s-process nucleosynthesis and the latest TP-AGB model, we calculate the degree of the overabundances of the intrinsic AGB star (the present white dwarf) at each ejection. Then, combining the accreting matter predicted by the model of wind accretion on successive occasions and mixing, we calculate the heavy-element overabundances of the barium star. The overabundance factor for nuclide i on the secondary star, g_i, is given by

$$g_i = \frac{M_{\text{env}} g_i^0 + \sum\limits_{n=1,m} f_i^n M_{\text{acc}}^n}{M_{\text{env}} + \sum\limits_{n=1,m} M_{\text{acc}}^n}, \quad (7)$$

where M_{env} is the mass of the outer envelope of barium star, M_{acc}^n is the mass accreted by barium star during the period of the n-th ejection of the intrinsic star, and f_i^n is the overabundance factor of the nuclide i of the intrinsic AGB star on that occasion. m is the total ejecting number undergone by the intrinsic AGB star. g_i^0 is the overabundance factor of nuclide i of barium star before the mass accretion. In the above formula we have assumed that the accreting matter has already completely mixed with the outer convective envelope of barium star.

We take as standard case: $M_{1,0}=3.0M_{\odot}$, $M_{2,0}=1.3M_{\odot}$, $v_{\rm ej}=15$ km s^{-1} and 0.15 times of the Bondi-Hoyle's accretion rate.

4. Results and analysis

4.1. The intrinsic AGB stars

Using the recent evolutionary model and nucleosynthesis scenario of intrinsic TP-AGB stars (Straniero et al. 1995; Straniero et al. 1997; Gallino et al. 1998), we calculate the heavy-element abundances on the surface of solar metallicity $3M_{\odot}$ AGB star with wind mass loss. The TDU begins at the 8th pulse. The average heavy element abundances on the surface are given in Fig. 1.

In Fig. 1, the abscissa represents the average logarithmic ratio of the abundances of the heavier s-elements Ba, La, Nd, and Sm ('hs') to the lighter s-elements Y and Zr ('ls'), which depends on the neutron exposure. The ordinate is the logarithmic enhancement in 'ls' with respect to iron in the envelope, which is closely related to the synthesis in the He-intershell and the dilution factor. The different curves represent the results of different neutron exposures.

Indeed, the neutron exposures of ^{22}Ne in different thermal pulses have been showed in Sect. 3.1. In calculation, we adjust the neutron exposure of ^{13}C source. Gallino et al (1998) suggested the ^{13}C profile in ^{13}C pocket by their Fig. 1, namely their 'standard' case. Then they showed that the resulting heavy-elements abundances were nonsolar by their Fig. 14, while simply increasing the previously adopted abundance of ^{13}C by a factor of 2 could reproduce the main component of solar system (see their Fig. 16). Here, instead of the abundance of ^{13}C, we adjust the total neutron exposure caused by ^{13}C source to calculate the nucleosynthesis of AGB stars. Thus, the different values of 'a' in our Fig. 1 represent the different times of the actual total neutron exposures to the 'standard' case suggested by Gallino et al. (1998). Our result of $a=1.0$ corresponds to the 'standard' case of Gallino et al. (1998), and the $a=1.5$ case corresponds to their results of increasing the previously adopted abundance of ^{13}C by a factor of 2. In reality, Gallino et al. (1998) have illustrated this times relationship (1.5 vs. 2) in the description and discussion about their Figs. 14, 15 and 16.

Our Fig. 1 shows that our results are very similar to those of Gallino et al. (1998). The curve with $a=1.0$ exhibits clearly that the abundances of the heavier nuclei are lower than those of the lighter nuclei in the 23rd interpulse phase like Gallino et al. (1998), namely [hs/ls]<0.0 (the abscissa), which means that this case can not reproduce the solar abundance distribution due to a lower production for heavier nuclei. While the curve with $a=1.5$ produces [hs/ls]∼0.0 in the 23rd interpulse phase, which means that the abundances of the heavier and the lighter nuclei are solar like. So, our 'average' heavy-element abundances on the surfaces of AGB stars can fit the detailed abundance distribution of nuclei obtained by Gallino et al. (1998). In addition, we should note that, because we neglect the effects of light neutron poisons on nucleosynthesis in calculation, our 'a' values are slightly higher than the corresponding case of Gallino et al. (1998).
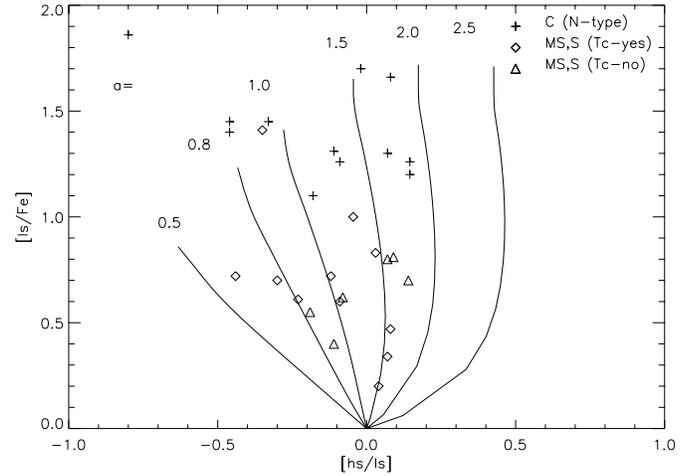

Fig. 1. Comparison of the theoretical predictions of surface heavy-element abundances for different neutron exposures (solid lines) with observations of intrinsic AGB stars. The numbers of 'a' represent the times of the corresponding exposures in the ^{13}C profile suggested by the Fig. 1 of Gallino et al. (1998).

We calculate some other curves with different a values, which are given in Fig. 1 too. The results show that all of our available observational data are compatible with the range $0.5{\leq}a{\leq}2.0$. The evolutionary curves for three cases ($a=1.0$, 1.5, 2.0) move upward as the dredge-ups proceed, and from the region of MS, S stars to reach the region of the carbon stars (symbol plus). And the larger neutron exposure, the higher [hs/ls] ratio will be, which means the large neutron exposure benefits the production of the heavier s-process elements.

^{12}C isotope in the He-intershell of TP-AGB stars, together with the s-process elements, is dredged-up and mixed to the envelope by the TDU process, which causes that the C/O ratio on the surface increases gradually with the thermal pulses. The increase correlates to the overabundances of heavy-elements. Our Fig. 2 displays the relationship of heavy-element abundances to C/O ratio. The values of 'a' are relevant to the values in Fig. 1. From the beginning of TDU, the values of C/O ratio and heavy-element abundances increase gradually. After some dredge-ups, C/O becomes greater than 1, that is, the star become carbon star ($a=1.2$, 1.5, 2.5). The different curves show that the higher neutron exposure, the more heavy elements are produced.

The results of Fig. 1 and Fig. 2 illustrate that, adopting the new TP-AGB nucleosynthesis scenario, choosing the reasonable parameters, we can explain the observed heavy-element abundances and C/O ratio of MS, S and C (N-type) stars. Also, we can explain the M→S→C evolutionary sequence on the basis of the lighter−heavier s-element abundances relationship and the heavy-element abundances−C/O ratio relationship simultaneously.

4.2. The barium stars

Our model assumes that the binary system remains always detached, so that the only interaction between the two compo-
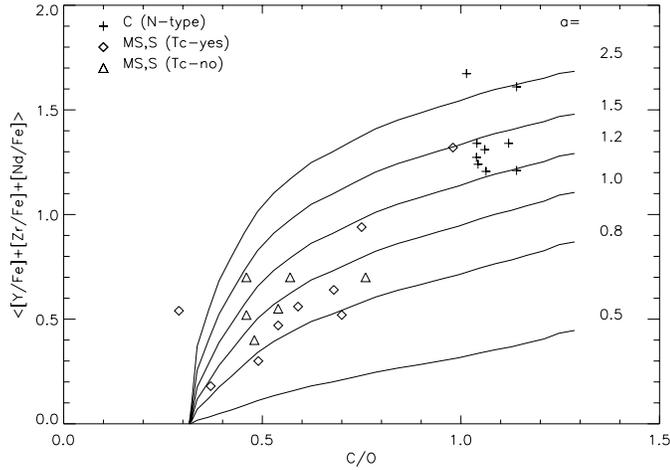
Fig. 2. Comparison of theoretical predictions of the relationships between heavy-element abundances and C/O ratios for different neutron exposures (solid lines) with observations of intrinsic AGB stars. The numbers of 'a'represent the same meanings as in Fig. 1.

Fig. 3. Comparison of the predicted to observed relationships of surface heavy-element abundances to the orbital periods of barium stars corresponding to different neutron exposures of intrinsic AGB stars (solid lines) in standard case of wind accretion. The numbers represent the same meanings as in Fig. 1.

nents of the binary system occurs via the accretion by the less evolved component of some fraction of the mass lost through stellar wind by the carbon- and heavy elements-rich AGB component. In other words, the internal structure of each component remains unaffected by the presence of its companion, so that the usual structural properties of single stars remain valid. Based the above-mentioned model, the heavy-element abundances of intrinsic AGB stars are calculated firstly, then the heavy-element overabundances of barium stars are self-consistently calculated through the progressive pulsed wind accretion and mixing.

The change equations of orbital elements are obtained by adopting the angular momentum conservation of the total system (including the two companions and the ejected matter) (see Sect. 3.2.1 and Appendix).

The observed orbital periods of 14 barium stars are in the range of 80.53 to 6489 days. According to the discussions of Jorissen et al. (1998) and Zhang et al. (1999), the barium stars with orbital period $P > 1500$ or $P > 1600$ d formed through wind accretion, while those with $P < 600$ d formed through other scenarios. So in calculation, we adopt 600-7000 d to be the orbital period range of wind accretion.

The actual mass accretion rate between the components of binary systems can be 0.1-1 times of B-H rate (Boffin & Začs 1994), while SPH simulation (Theuns et al. 1996) indicated that the actual rate was about 10 times smaller than B-H rate. We adopt 0.15 times of B-H rate as the standard case in our calculation.

The calculated relationships between the heavy-element overabundances [s/Fe] and orbital period P of barium stars are displayed in Fig. 3, which are based on the standard case of wind accretion. Here, again, the various curves correspond to different times of the neutron exposures of the intrinsic AGB stars, and 'a' represents the same meanings as in Fig. 1 and Fig. 2. Every point of every curve refers to the different orbital period, within the range 600-7000 d. Since the shorter the or-
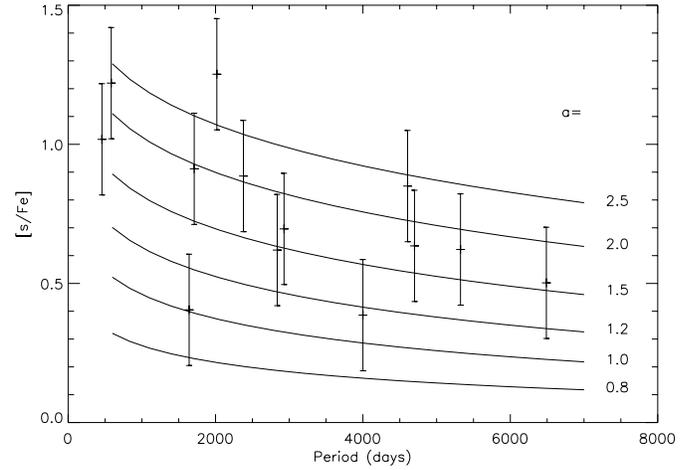
bital period, the greater the accretion, and hence the larger the heavy-element overabundances will be. For the curves in Fig. 3, the higher points correspond to the shorter periods. The theoretical results with $0.8 \le a \le 2.5$ can fit the observations within the error range.

To make further examination to the dependence of heavy-element abundances on the angular momentum conservation model of wind accretion, the mass accretion scenario of barium stars is analyzed carefully by comparing the predicted heavy-element overabundances of different atomic charge Z with the observations of 14 barium stars.

In calculation, we try to make the calculated eccentricity e and orbital period P match to the observations of the barium stars. The results are given in Fig. 4a-n. The corresponding neutron exposure of intrinsic AGB components, a, and the orbital period P of barium stars are exhibited in the every Figure.

These results show that, for the 9 long-period barium stars ($P > 1600$ d), the calculated curves can fit well to the observed heavy-element abundances in the error range (see Fig. 4a-i) according to the standard case of our wind accretion scenario. For the two classical barium giant stars HD 204075 (ζ Cap) and HD 16458 (HR 774), the results will fit the observations better after the mass accretion rate is improved to 0.5 times as much as the B-H accretion rate (see Fig. 4j and k). For the three barium stars with shorter orbital periods, HD 199939, HD 46407 and HD 77247 (the orbital periods are 584.9, 457.4 and 80.53 days respectively), the calculations can not fit the observations (see Fig. 4l-n).

Because the same program barium stars are chosen in Fig. 4 as in Fig. 3, the reasonable result would be that the same observational sample should correspond to the same neutron exposure of intrinsic AGB stars in the two figures. The results are advantageous to the standpoint: for most of barium stars, the corresponding neutron exposures of 'a' in Fig. 4a-n are consistent to

the values of 'a' in Fig. 3 within the error ranges. Namely, the comparisons between the predicted and the observed results are basically identical in the heavy-element abundances diagram and the heavy-element abundance−orbital period P diagram of barium stars.

Comparisons between the predicted and the observed abundances of barium stars in Fig. 3 and Fig. 4 show that the barium stars with longer orbital period (P>1600 d) form through wind accretion, and the change range of mass accretion rate should be 0.1 to 0.5 times as much as the Bondi-Hoyle's accretion rate; the barium stars with shorter period (P<600 d) can form through other scenarios: stable case C disk accretion or common envelope ejection. Our results support quantitatively the conclusions of Jorissen et al. (1998) and Zhang et al. (1999).

5. Conclusion and discussion

5.1. The intrinsic AGB stars

Adopting the latest AGB stars evolutionary theory and nucleosynthesis scenario, the heavy-element abundances of solar metallicity $3M_\odot$ AGB stars are calculated. It is shown that, adopting reasonable parameters, the calculated results of the heavier/lighter s-elements ratio− overabundance relationships and the C/O ratio−overabundance relationships can fit the observations. The evolution of AGB stars along the M→S→C sequence is thus further explained from the evolutionary theories and heavy-elements nucleosynthesis of AGB stars. A $3M_\odot$ AGB star will undergo about 27 pulses before it becomes carbon star.

The results showed that the overabundances of s-process elements depend significantly on the neutron exposure: for the lower neutron exposures (a<1.5), the lighter s-process elements are more abundant than the heavier ([hs/ls]<0.0); for the higher neutron exposures (a>1.5), the latter can increase strongly with the increase of neutron exposures, and the lighter s-process elements change slightly ([hs/ls]>0.0); while the results with a=1.5 can explain the solar heavy-element abundance distribution, which confirm the results of Gallino et al. (1998). Moreover, ^{12}C abundance correlates to the s-process element abundances. Both C/O ratio and s-element abundances increase with the occurrence of TDU. After some dredge-ups, C/O ratio reaches 1, from which the AGB stars become carbon stars. The observed MS, S and C (N-type) stars lie in a range of neutron exposure: a=0.5-2.5. The over low neutron exposure can not produce carbon stars (e.g. a=0.5). Our calculation thus provides a further theoretical basis for the evolution of AGB stars along the M→S→C sequence based on the heavy-element abundances and C/O ratio. The general agreements between our calculations and the observations indicate that we adopt reasonable parameters and theories of evolution and nucleosynthesis of AGB stars in calculation.

The stars with initial main sequence mass 1.5−$4M_\odot$ can form carbon stars (Groenewegen et al. 1995). We consider only a $3M_\odot$ star model in our calculation. So the comparison between the calculated results and the observations is somewhat rough. With further studies of the evolutionary theory of AGB
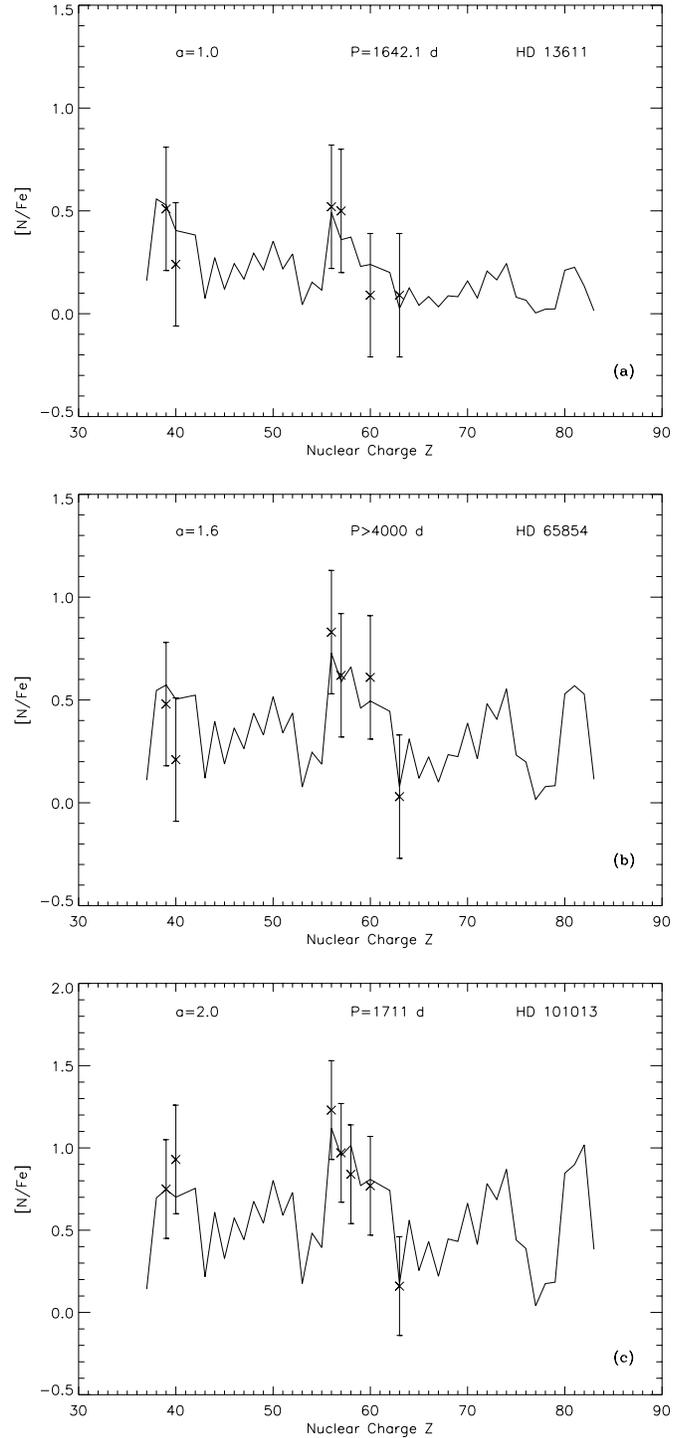

Fig. 4a–c. The fitting of the predicted to observed heavy-element abundances of 14 barium stars in standard case of wind accretion. But the curves in Fig. 4j and k represent the results of higher accretion rate: 0.5 times of the Bondi-Hoyle's rate. In every figure, the alphabet 'a' represents the times of the corresponding neutron exposure in the ^{13}C profile suggested by the Fig. 1 of Gallino et al. (1998), and 'P' represents the orbital period of the barium star.
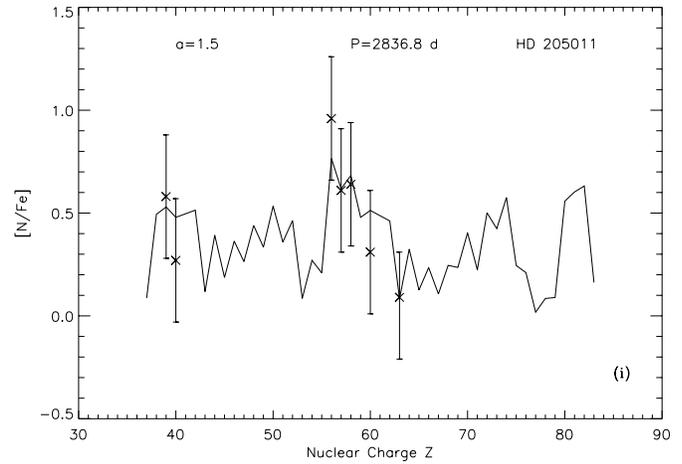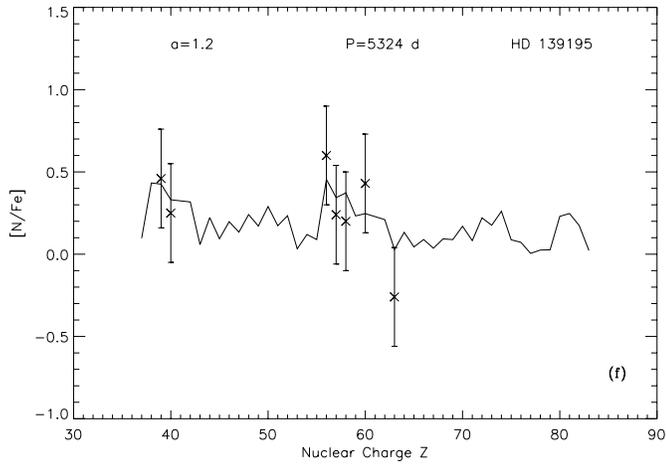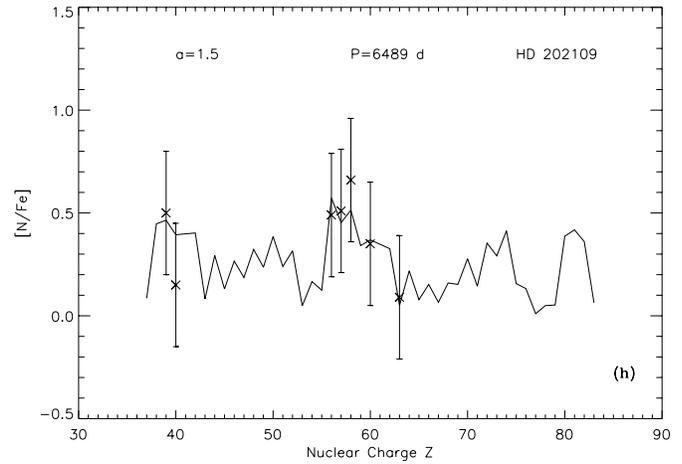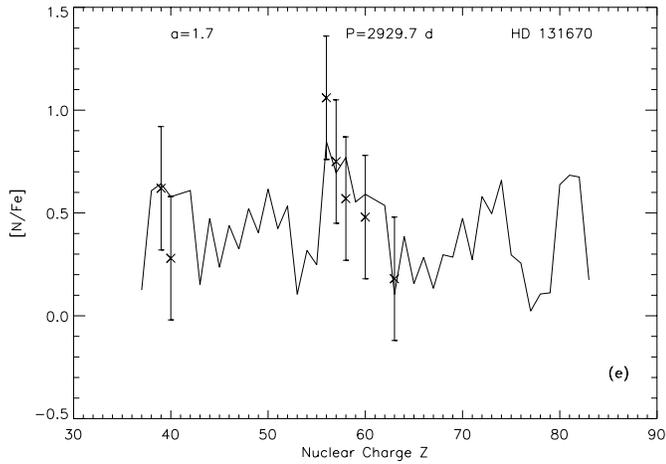
Fig. 4d–f.

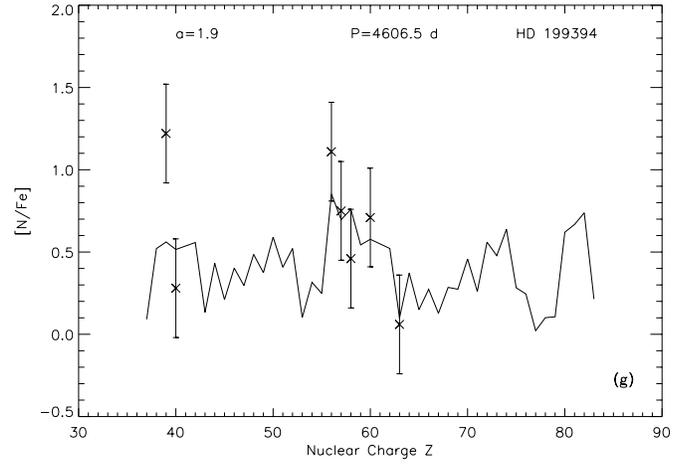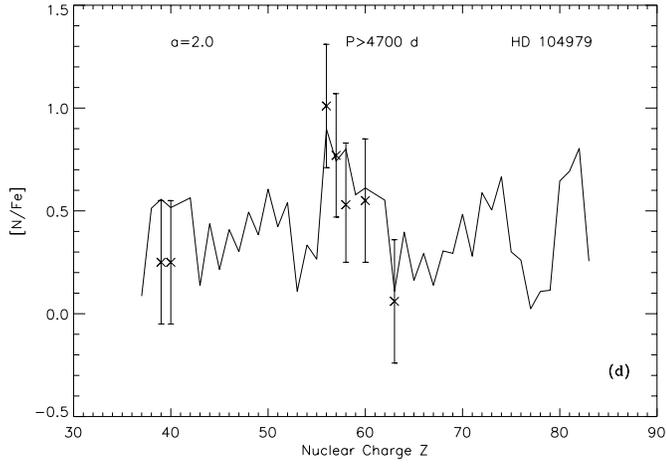**Fig. 4g–i.**

stars and increasing observational data, we can expect a deeper understanding on the nucleosynthesis of AGB stars.

5.2. The barium stars

Taking the conservation of angular momentum in place of the conservation of tangential momentum for wind accretion sce-

nario, considering the change of $\delta r/r$ term, and not neglecting the square and higher power terms of eccentricity, the change equations of orbital elements are recalculated. We combine wind accretion with the nucleosynthesis of intrinsic AGB stars, to calculate, in a self-consistent manner, the heavy-element overabundances of barium stars through mass accretion during successive pulsed ejection, followed by mixing.
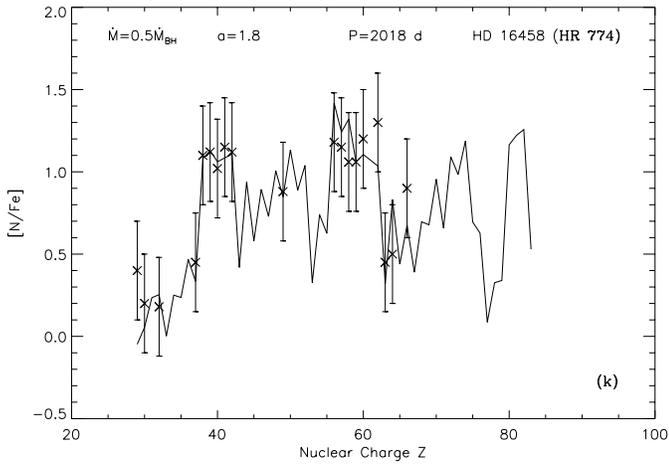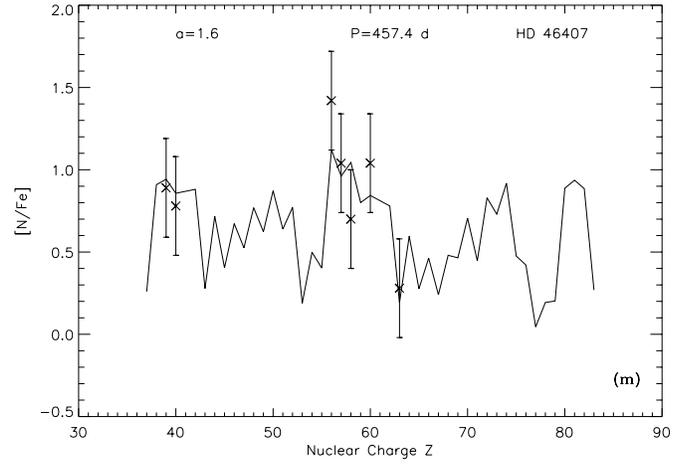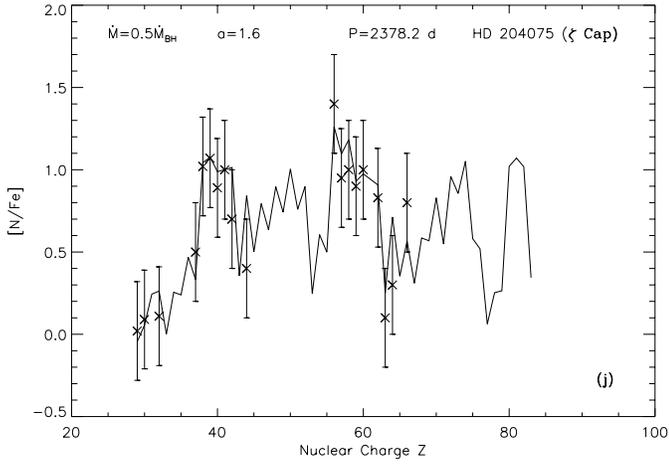
Fig. 4j–l.

Fig. 4m and n.
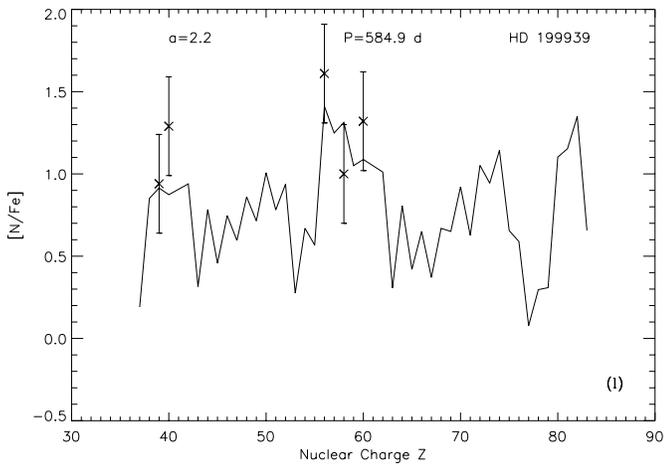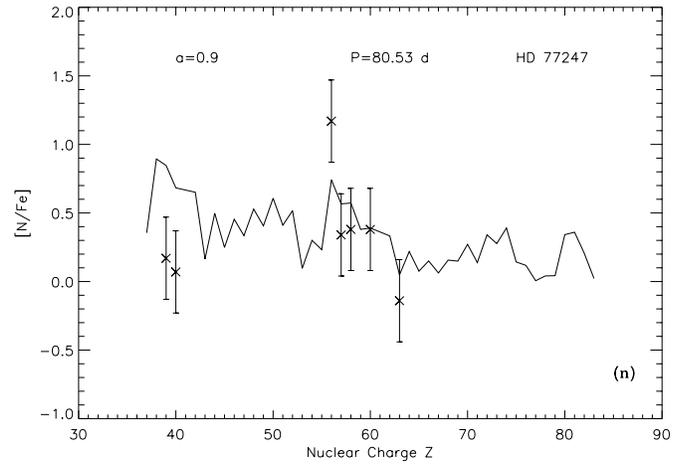
The calculated relationships of heavy-element abundances − orbital period P can fit the observations within the error ranges. Moreover, the predictions of the detailed abundances of different atomic charge Z can match well the observations of 11 program barium stars with longer orbital period ($P>1600$ d). The corresponding neutron exposures are in the range of $0.8<a<2.5$. The higher neutron exposure (e.g. $a=2.0$) will pro-

duce the more abundant the heavier s-elements than the lighter (see Fig. 4c); on the contrary, the abundances of the lighter s-elements are higher than the heavier with low neutron exposure (e.g. $a=1.0$, see Fig. 4a); while $a=1.5$ will produce the almost equal abundances of the heavier to the lighter s-elements (see Fig. 4h). These neutron exposures can fit the corresponding results of intrinsic AGB stars. Naturally, we can understand the observations of no-Tc MS and S stars, which are commonly believed to be the descendants of barium stars. These results of the extrinsic AGB stars confirm the reliability of the nucleosynthesis and evolution of intrinsic AGB stars. Simultaneously, the results confirm that our wind accretion model and parameters adopted are suitable.

Analyzing our results, we understand that the barium stars with longer orbital period ($P>1600$ d) form through wind accretion. Those with shorter orbital period ($P<600$ d) form through other scenarios, such as dynamically stable late case C mass transfer or common envelope ejection. Moreover, the change range of mass accretion rate should be 0.1 to 0.5 times as much as the Bondi-Hoyle's accretion rate. The corresponding range of orbital periods and mass accretion rate to the formation of barium stars still need to be tested by more observations.

At present, the orbital elements of a large sample barium stars, Tc-poor S stars have been published (Udry et al. 1998a, 1998b; Carquillat et al. 1998). But the corresponding heavy-element abundances have not been obtained. So we need the high resolution, high signal-to-noise spectral observations of these stars, which are combined with the observations of orbital elements, to research their characters and formation.

In addition, we should note that metallicity is an important factor to the AGB stars nucleosynthesis and the formation of chemical peculiar stars. Actually, ^{13}C neutron source is related to the metallicity (Busso et al. 1995, 1999 and references therein; Gallino et al. 1999). Gallino et al. (1998) calculated the s-element nucleosynthesis of $2M_\odot$ AGB stars with low metallicity $Z=0.01$, and obtained similar abundance distribution to the $3M_\odot$ with solar metallicity AGB stars model. Busso et al. (1999) and Zhang et al. (1998b) have discussed the inverse correlation between the heavy-element abundances and the metallicity [Fe/H] of intrinsic and extrinsic AGB stars. Also, the nucleosynthesis results of low metallicity AGB stars are more suitable to study the Galactic chemical evolution in the early stage of the Galaxy. For extrinsic AGB stars, Jorissen et al. (1998) suggested that the s-process operation was more efficient in a low-metallicity population, so the Pop. II CH stars may has accreted the material much enriched in heavy elements from the former AGB companion. In this paper, our main aims are (1) calculating the AGB stars nucleosynthesis, so that we can explain the observed heavy-element abundances of MS, S and C (N-type) stars, which are near solar metallicity, and supply evidence to the M→S→C evolutionary sequence; (2) discussing the wind accretion scenario of Ba stars, which are near solar metallicity too (Začs 1994; Smith et al. 1993). So we only calculate the solar metallicity case. We will extend to study the low metallicity case in the forthcoming paper.

Appendix: the angular momentum conservation model of wind accretion for barium stars: equations

For the binary system, the two components (an intrinsic AGB star with mass M_1, the present white dwarf, and a main sequence star with mass M_2, the present barium star) rotating around the mass core C, so the total angular momentum is conservative in the mass core reference frame. If the two components exchange material through wind accretion, the angular momentum conservation of total system is showed by:

$$\Delta(\mu r^2 \dot\theta) = \omega r_1^2 (\Delta M_1 + \Delta M_2) + r_2 v(\Delta M_1 + \Delta M_2), \quad (8)$$

where μ is reduced mass, and r is the distance from M_2 to M_1. r_1 and r_2 are the distances from M_1, M_2 to the mass

core C respectively. ω $(=2\pi/P)$ is angular velocity, where $P = 2\pi A^2 (1-e^2)^{\frac{1}{2}}/h$ is the orbital period (Huang 1956). v is an additional effective velocity defined through the angular momentum variation in the direction of orbital motion of component 2. The first term on the right side of the equal-sign is the angular momentum lost by the escaping material and the second term is the additional angular momentum lost by the escaping material.

For the binary system, according to Huang (1956), the changes of orbital elements, the orbital semi-major axis A and eccentricity e, are

$$\frac{\Delta A}{A} = \frac{\Delta(M_1+M_2)}{M_1+M_2} - \frac{\Delta E}{E}, \quad (9)$$

$$\frac{e\Delta e}{1-e^2} = \frac{\Delta(M_1+M_2)}{M_1+M_2} - \frac{1}{2}\frac{\Delta E}{E} - \frac{\Delta h}{h}, \quad (10)$$

where

$$\begin{aligned}\frac{\Delta E}{E} &= \frac{\Delta T}{E} + \frac{\Delta\Omega}{E} \\ &= \frac{r\dot\theta}{E}\Delta(r\dot\theta) + \left[\frac{\Delta(M_1+M_2)}{M_1+M_2}\frac{2A}{r} - \frac{2A\Delta r}{r^2}\right].\end{aligned} \quad (11)$$

According to the angular momentum conservation model, the $\Delta(r\dot\theta)$ term can be obtained from the following equation:

$$\begin{aligned}\frac{M_1 M_2}{M_1+M_2} r\Delta(r\dot\theta) &= \Delta\left(\frac{M_1 M_2}{M_1+M_2} r\, r\dot\theta\right) \\ &\quad - \Delta\left(\frac{M_1 M_2}{M_1+M_2} r\right) r\dot\theta \\ &= \Delta(\mu r^2 \dot\theta) - \Delta\left(\frac{M_1 M_2}{M_1+M_2} r\right) r\dot\theta \\ &= \omega r_1^2 (\Delta M_1 + \Delta M_2) \\ &\quad + r_2 v(\Delta M_1 + \Delta M_2) \\ &\quad - \Delta\left(\frac{M_1 M_2}{M_1+M_2} r\right) r\dot\theta,\end{aligned} \quad (12)$$

thus

$$\begin{aligned}\Delta(r\dot\theta) &= -r\dot\theta\left[\frac{\Delta M_1}{M_1} + \frac{\Delta M_2}{M_2} - \frac{\Delta(M_1+M_2)}{M_1+M_2}\right] - r\dot\theta\frac{\Delta r}{r} \\ &\quad + \frac{\Delta(M_1+M_2)}{M_2}v + \frac{rG^{\frac{1}{2}}M_2\Delta(M_1+M_2)}{M_1(M_1+M_2)^{\frac{1}{2}}A^{\frac{3}{2}}},\end{aligned} \quad (13)$$

then, we can obtain

$$\begin{aligned}\frac{r\dot\theta\Delta(r\dot\theta)}{E} &= -\frac{(r\dot\theta)^2}{E}\left[\frac{\Delta M_1}{M_1} + \frac{\Delta M_2}{M_2} - \frac{\Delta(M_1+M_2)}{M_1+M_2}\right] \\ &\quad - \frac{r\dot\theta^2}{E}\Delta r + \frac{r\dot\theta}{E}\frac{\Delta(M_1+M_2)}{M_2}v \\ &\quad + \frac{r^2\dot\theta}{E}\frac{G^{\frac{1}{2}}M_2\Delta(M_1+M_2)}{M_1(M_1+M_2)^{\frac{1}{2}}A^{\frac{3}{2}}} \\ &= 2(1-e^2)^{\frac{1}{2}}\left[\frac{\Delta M_1}{M_1} + \frac{\Delta M_2}{M_2}\right]\end{aligned}$$

$$- 2(1-e^2)^{\frac{1}{2}}\frac{\Delta(M_1+M_2)}{M_2}\frac{v}{v_{\mathrm{orb}}}$$

$$- 2(1-e^2)^{\frac{1}{2}}\frac{M_2\Delta(M_1+M_2)}{M_1(M_1+M_2)}$$

$$- 2(1-e^2)^{\frac{1}{2}}\frac{\Delta(M_1+M_2)}{M_1+M_2}+\frac{2\Delta r}{A(1-e^2)^{\frac{1}{2}}} \;. \quad (14)$$

Thus

$$\begin{aligned}
\frac{\Delta E}{E} =\; & 2(1-e^2)^{\frac{1}{2}}\left[\frac{\Delta M_1}{M_1}+\frac{\Delta M_2}{M_2}-\frac{\Delta(M_1+M_2)}{M_2}\frac{v}{v_{\mathrm{orb}}}\right]\\
& - 2(1-e^2)^{\frac{1}{2}}\frac{M_2\Delta(M_1+M_2)}{M_1(M_1+M_2)}\\
& + \left(2-2(1-e^2)^{\frac{1}{2}}\right)\frac{\Delta(M_1+M_2)}{M_1+M_2} \;.
\end{aligned} \quad (15)$$

The $\Delta h/h$ term is:

$$\begin{aligned}
\frac{\Delta h}{h} =\; & -\frac{\Delta M_1}{M_1}-\frac{\Delta M_2}{M_2}+\frac{2+e^2}{2(1-e^2)^{\frac{1}{2}}}\frac{\Delta(M_1+M_2)}{M_2}\frac{v}{v_{\mathrm{orb}}}\\
& + \frac{M_2\Delta(M_1+M_2)}{M_1(M_1+M_2)}+\frac{\Delta(M_1+M_2)}{M_1+M_2} \;.
\end{aligned} \quad (16)$$

Combining Eqs. (9), (10), (15) and (16), we can obtain the changes of orbital semi-major axis A and eccentricity e:

$$\begin{aligned}
\frac{\Delta A}{A} =\; & -2(1-e^2)^{\frac{1}{2}}\left[\frac{\Delta M_1}{M_1}+\frac{\Delta M_2}{M_2}-\frac{\Delta M_1+\Delta M_2}{M_2}\frac{v}{v_{\mathrm{orb}}}\right]\\
& + 2(1-e^2)^{\frac{1}{2}}\frac{M_2(\Delta M_1+\Delta M_2)}{M_1(M_1+M_2)}\\
& + \left[2(1-e^2)^{\frac{1}{2}}-1\right]\frac{\Delta M_1+\Delta M_2}{M_1+M_2},
\end{aligned} \quad (17)$$

$$\begin{aligned}
\frac{e\Delta e}{1-e^2} =\; & \left[1-(1-e^2)^{\frac{1}{2}}\right]\left[\frac{\Delta M_1}{M_1}+\frac{\Delta M_2}{M_2}-\frac{\Delta M_1+\Delta M_2}{M_1+M_2}\right]\\
& - \left[1-(1-e^2)^{\frac{1}{2}}\right]\frac{M_2(\Delta M_1+\Delta M_2)}{M_1(M_1+M_2)}\\
& - \frac{3e^2}{2(1-e^2)^{\frac{1}{2}}}\frac{\Delta M_1+\Delta M_2}{M_2}\frac{v}{v_{\mathrm{orb}}} \;.
\end{aligned} \quad (18)$$

References

Anders E., Grevesse N., 1989, Geochim. Cosmochim. Acta 53, 197

Arlandini C., Gallino R., Busso M., Straniero O., 1995, In: Noels A., Fraipont-Caro D., Gabriel M., Grevesse N., Demarque P. (eds.) Proc. 32d Liege Colloq., Stellar Evolution: What Should Be Done? Univ. de Liege, Liege, p. 447

Beer H., Voss F., Winters R.R., 1992, ApJS 80, 403

Boffin H.M.J., Jorissen A., 1988, A&A 205, 155

Boffin H.M.J., Začs L., 1994, A&A 291, 811

Bondi H., Hoyle F., 1944, MNRAS 104, 273

Boothroyd A.I., Sackmann I.J., 1988a, ApJ 328, 632

Boothroyd A.I., Sackmann I.J., 1988b, ApJ 328, 641

Boothroyd A.I., Sackmann I.J., 1988c, ApJ 328, 653

Boothroyd A.I., Sackmann I.J., 1988d, ApJ 328, 671

Burbidge E.M., Burbidge G.R., Fowler W.A., Hoyle F., 1957, Rev. Mod. Phys. 29, 547

Busso M., Gallino R., Lambert D.L., Raiteri C.M., Smith V.V., 1992, ApJ 399, 218

Busso M., Gallino R., Wasserburg G.J., 1999, ARA&A 37, 239

Busso M., Lambert D.L., Beglio L., et al., 1995, ApJ 446, 775

Cameron A.G.W., 1957, Chalk River Rep. CRL-41

Carquillat J.M., Jorissen A., Udry S., Ginestet N., 1998, A&AS 131, 49

Chang Rui-xiang, Zhang Bo, Peng Qiu-he, 1997, Chin. Astron. Astrophys. 21, 453

Gallino R., Arlandini C., Busso M., et al., 1998, ApJ 497, 388

Gallino R., Busso M., Lugaro M., Travaglio C., Vaglio P., 1999, In: Prantzos N., Harissopulos S. (eds.) Nuclei in the Cosmos V, Ed. Frontieres, Paris, p. 216

Groenewegen M.A.T., van den Hoek L.B., de Jong T., 1995, A&A 293, 381

Han Z., Eggleton P.P., Podsiadlowski P., Tout C.A., 1995, MNRAS 277, 1443

Herwig F., Blöcker T., Schönberner D., El Eid M., 1997, A&A 324, L81

Herwig F., Schönberner D., Blöcker T., 1998, A&A 340, L43

Hollowell D., Iben I. Jr., 1988, ApJ 333, L25

Huang S.S., 1956, AJ 61, 49

Iben I. Jr., 1975, ApJ, 196, 525

Iben I. Jr., 1977, ApJ 217, 788

Iben I. Jr., Renzini A., 1982a, ApJ 249, L79

Iben I. Jr., Renzini A., 1982b, ApJ 263, l23

Iben I. Jr., Tutukov A.V., 1985, ApJS 58, 661

Jorissen A., 1999, In: Le Bertre T., Lébre A., Waelkens C. (eds.) Asymptotic Giant Branch Stars. IAU Symp. 191, ASP, p. 437

Jorissen A., Mayor M., 1992, A&A 260, 115

Jorissen A., Van Eck S., 2000, In: Wing R.F. (ed.) The Carbon Star Phenomenon. IAU Symp. 177, ASP, San Francisco, astro-ph/9708052

Jorissen A., Van Eck S., Mayor M., Udry S., 1998, A&A 332, 877

Lambert D.L., 1991, In: Michaud G., Tutukov A. (eds.) Evolution of Stars: The Photospheric Abundance Connection. Kluwer, Dordrecht, p. 299

Lambert D.L., Gustafsson B., Eriksson K., Hinkle K.H., 1986, ApJS 62, 373

Lambert D.L., Smith V.V., Busso M., Gallino R., Straniero O., 1995, ApJ 450, 302

Liang Yan-chun, Zhang Bo, Peng Qiu-he, 1999, Acta Astrophysica Sinica 19, 213

Liu Junhong, Zhang Bo, Liang Yanchun, Peng Qiuhe, 2000, A&A in press

McClure R.D., Fletcher J.M., Nemec J.M., 1980, ApJ 238, L35

McClure R.D., Woodsworth A.W., 1990, ApJ 352, 709

Paczynski B., 1976, In: Eggleton P.P., Mitton S., Whelan J. (eds.) IAU Symp. 73, Structure and Evolution of Close Binary Systems. Reidel, Dordrecht, p. 75

Reimers D., 1975, In: Bascheck B., Kegel W.H., Traving G. (eds.) Problems in Stellar Atmospheres and Envelopes. Springer, Berlin, p. 229

Renzini A., Voli M., 1981, A&A 94, 175

Ruffert M., Arnett D., 1994, ApJ 427, 351

Smith V.V., Coleman H., Lambert D.L., 1993, ApJ 417, 287

Smith V.V., Lambert D.L., 1985, ApJ 294, 326

Smith V.V., Lambert D.L., 1986, ApJ 311, 843

Smith V.V., Lambert D.L., 1990, ApJS 72, 387

Straniero O., Chieffi A., Limongi M., Busso M., Gallino R., Arlandini C., 1997, ApJ 478, 332

Straniero O., Gallino R., Busso M., et al., 1995, ApJ 440, L85

Takahashi K., Yokoi K., 1987 At. Data Nucl. Data Tables 36, 375

Theuns T., Boffin H.M.J., Jorissen A., 1996, MNRAS 280, 1264

Tomkin J., Lambert D., 1986, ApJ 311, 819

Truran J.W., Iben I. Jr., 1977, ApJS 216, 797

Udry S., Jorissen A., Mayor M., Van Eck S., 1998a, A&AS 131, 25

Udry S., Mayor M., Van Eck S., Jorissen A., et al., 1998b, A&AS 131, 43

Utsumi K., 1985, In: Jaschek M., Keenan P.C. (eds.) Cool Stars with Excesses of Heavy Elements. Reidel, Dordrecht, p. 243

Začs L., 1994, A&A 283, 937

Zhang Bo, Chang Rui-xiang, Peng Qiu-he, 1998a, Chin. Astron. Astrophys. 22, 49

Zhang Bo, Liu Jun-hong, Liang Yan-chun, Peng Qiu-he, 1998b, Chin. Phys. Letter 15, 77

Zhang Bo, Liu Jun-hong, Liang Yan-chun, Peng Qiu-he, 1999, Chin. Astron. Astrophys. 23, 189